CLIMATOLOGY

Tropical cyclone motion in a changing climate

Gan Zhang[1,2]*, Hiroyuki Murakami[2,3,4], Thomas R. Knutson[2], Ryo Mizuta[4], Kohei Yoshida[4]

The locally accumulated damage by tropical cyclones (TCs) can intensify substantially when these cyclones move more slowly. While some observational evidence suggests that TC motion might have slowed significantly since the mid-20th century (*1*), the robustness of the observed trend and its relation to anthropogenic warming have not been firmly established (*2–4*). Using large-ensemble simulations that directly simulate TC activity, we show that future anthropogenic warming can lead to a robust slowing of TC motion, particularly in the midlatitudes. The slowdown there is related to a poleward shift of the midlatitude westerlies, which has been projected by various climate models. Although the model's simulation of historical TC motion trends suggests that the attribution of the observed trends of TC motion to anthropogenic forcings remains uncertain, our findings suggest that 21st-century anthropogenic warming could decelerate TC motion near populated midlatitude regions in Asia and North America, potentially compounding future TC-related damages.

INTRODUCTION

Tropical cyclone (TC) motion is a central issue for prediction and mitigation efforts, as it affects the location of storm-related damages (*5*). For a specific location, the accumulated damage by TCs can intensify significantly when TCs move slowly. Examples of such damage intensification include recent Atlantic Hurricanes Harvey (2017), Florence (2018), and Dorian (2019). These high-impact cases also raise concerns regarding slow-moving TCs in the future climate. While it now appears unlikely that observed TC motion slowed significantly on the global scale since the mid-20th century (*1–4*), there is some evidence for a slowing of TC motion over the continental United States since 1900 (*4*). However, the relationship of TC motion decreases to anthropogenic forcing has not been firmly established (*2*, *3*).

TC motion is regulated by multiple factors (*6–10*), with the large-scale atmospheric circulation often being the leading control (*5*). Recent observational studies (*1*, *11*) proposed that TC motion has been affected by the weakening of the large-scale circulation in recent decades, possibly driven by anthropogenic warming. Large-scale circulation weakening with warming could possibly arise from various physical mechanisms. For example, the tropical overturning circulation is simulated to weaken with greenhouse gas–induced warming because of an enhancement of radiative cooling and atmospheric stability (*12*), as well as because of the moistening of the atmosphere (*13*). Meanwhile, the extratropical circulation may weaken because of a reduction of the pole-to-equator temperature gradient related to the amplified Arctic warming (*14–16*). Nonetheless, there remain substantial uncertainties in (i) whether the anthropogenic warming has driven detectable changes (e.g., weakening) of atmospheric circulation in the tropics or the Northern Hemisphere extratropics (*17–19*) and (ii) how future anthropogenic warming might affect the large-scale circulation, especially on the regional scale (*20–22*). These uncertainties, along with the inhomogeneity of TC observations (*2–4*, *23*), warrant further examination in connection with TC motion and the anthropogenic warming.

[1]Atmospheric and Oceanic Sciences Program, Princeton University, Princeton, NJ, USA. [2]Geophysical Fluid Dynamics Laboratory, National Oceanic and Atmospheric Administration, Princeton, NJ, USA. [3]University Corporation for Atmospheric Research, Boulder, CO, USA. [4]Meteorological Research Institute, Tsukuba, Japan.
*Corresponding author. Email: ganzhang@princeton.edu

The recent development of TC-permitting global and regional climate simulations offers opportunities to study TC activity under changing climate conditions. The confidence in these applications builds on the performance of the dynamical models in simulating and predicting real-world TC activity (*24*, *25*). The dynamical models can also offer insights into unforced internal variability of the climate system (*26*), which arises from intrinsic processes and their interactions. Previous studies show that unforced atmospheric and/or unforced coupled atmosphere-ocean variability can profoundly affect the large-scale circulation (*27*) and TC activity (*28*, *29*) on various time scales. Such variability may obscure or potentially dominate over climate responses to external factors, including anthropogenic forcing, depending on the variable, time scale, and region. Nonetheless, robust simulated climate responses to external forcing can be obtained from models using a large number of individual simulations, namely, the large-ensemble simulation (*27*). However, the constraint of computing resources often limits the application of the large-ensemble simulation technique at a TC-permitting resolution.

Here, we investigate the relation between TC motion and the large-scale circulation using a unique set of high-resolution and large-ensemble simulations. The simulations can reproduce some aspects of historical TC activity (*30*) and consist of 90 to 100 individual simulations for historical (1951–2010) conditions, early 20th-century conditions, and future climate scenarios (*31*). More details of the model and the experiment settings are available in Methods. Because the large-ensemble simulation generates reasonably realistic climate (*31*) and TC activity (*30*), it is potentially useful for investigating impacts of historical boundary conditions [including sea surface temperature (SST) variability, aerosols, and greenhouse gases] and unforced atmospheric variability on TC activity. The simulations can help to cast light on whether multidecadal SST variability and trends, as well as anthropogenic warming, can alter TC motion via the large-scale circulation.

RESULTS

Evaluation of large-ensemble simulations

We first evaluate the large-ensemble simulation of TC motion and its relationship with the large-scale circulation (Fig. 1). The climatology of TC motion in the observation and the historical (1951–2010)

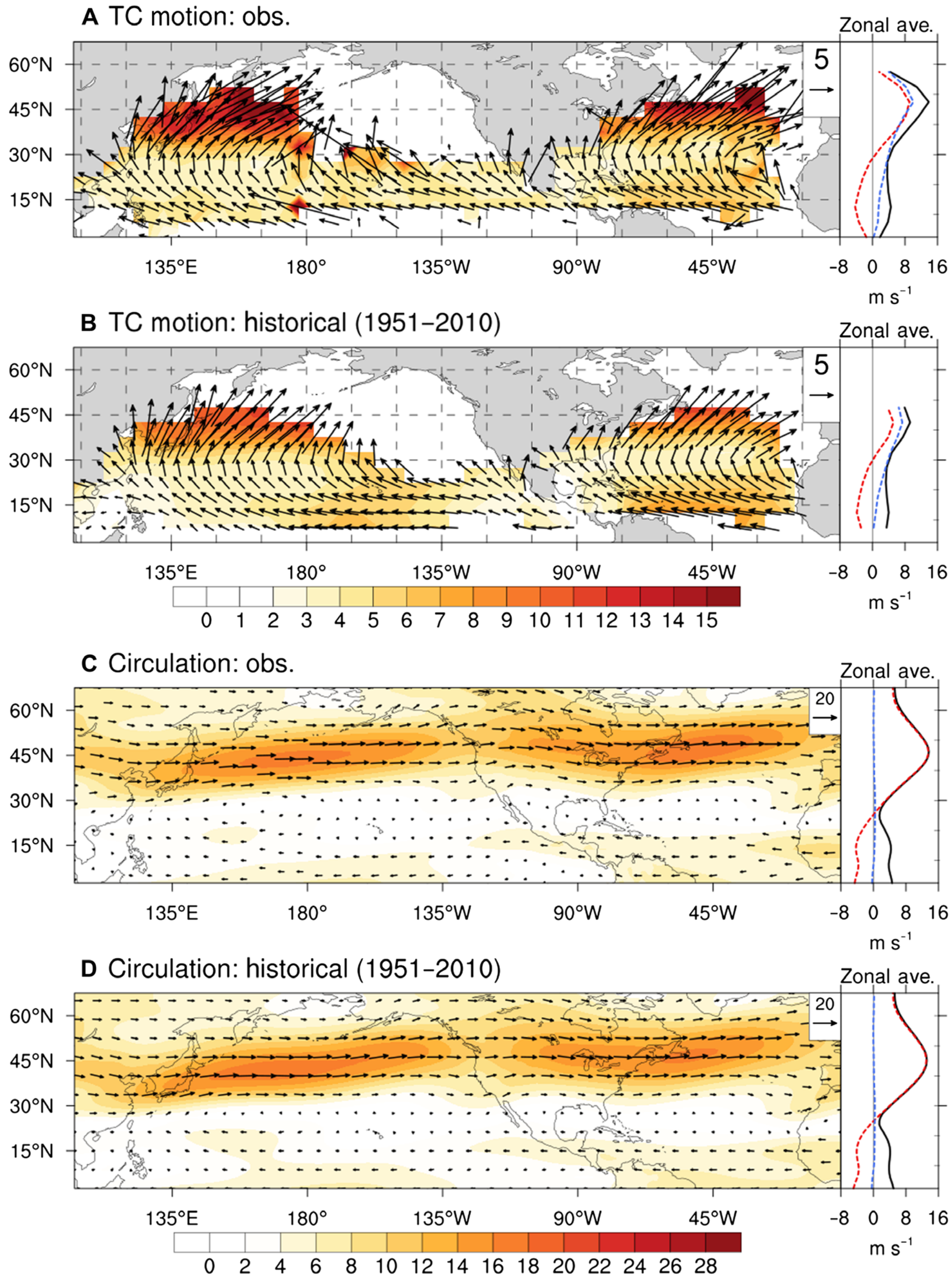

Fig. 1. Observed and simulated climatology of TC motion (m s^{-1}) and midtropospheric TC-steering circulation (m s^{-1}) during July to October (1951–2010). (**A**) TC motion vector from the International Best Track Archive for Climate Stewardship (IBTrACS) data. (**B**) TC motion vectors in the large-ensemble historical simulation. (**C**) Midtropospheric (500-hPa) winds from the CERA-20C data. (**D**) Midtropospheric (500-hPa) wind from the large-ensemble historical simulation. Color shading depicts translation speed (A and B) or wind speed (C and D). The right panels show the zonally averaged climatology of speed magnitude (black), as well as zonal vector (red) and meridional vector (blue) of TC motion (A and D) and midtropospheric winds (C and D).

simulation show consistent patterns. As in the observation, higher translation speeds in the simulation appear in the midlatitudes (>30°N), followed by parts of the tropics (10°N to 20°N), while the lowest mean translation speeds are generally located in the subtropics (20°N to 30°N). The TC observations are slightly noisier and show faster TC motion north of 40°N than in the simulations. This difference might arise from potential model biases and/or differences in the TC-tracking methods (see Methods). Besides TC motion, the observations and historical (1951–2010) simulations also show good agreement in the large-scale circulation.

The vortex-flow interaction can affect TC motion in some complex and even counterintuitive ways. For example, a reduction of extratropical weather perturbations can slow TC motion, especially in the meridional direction (*10*), and a purely zonal environmental wind that varies latitudinally like the midlatitude jet can deflect TCs poleward (*7*, *8*). Nonetheless, as a first-order approximation, the speed of TC motion is positively correlated with the background midtropospheric wind speed (*5*, *6*). For example, the relatively fast TC motion in the extratropics coincides with the strong westerly winds related to the midlatitude jet. The positive correlation in the observational data is overall well represented by the large-ensemble simulation (fig. S1). The fidelity of the large-ensemble simulation in representing TC motion and the large-circulation lays the foundation for further analyses.

Changes of TC motion and large-scale circulation

We now examine the changes of TC motion forced by historical (1951 to 2010) conditions (including SST, greenhouse gases, and aerosols) and future anthropogenic warming (Fig. 2, A and B). For TC motion, the differences between the idealized early 20th century and the historical (1951 to 2010) climates are generally small (<1 m s^{-1}; Fig. 2A). The differences suggest that historical SST trends over the 20th century, together with greenhouse gases, may have contributed to an acceleration of TC motion in the tropics but only a weak deceleration in limited extratropical regions. Therefore, the simulated historical changes, at least by the models examined by this study (Fig. 2A and figs. S8 to S9), are inconsistent with the notion that anthropogenic forcing has caused a significant slowdown of TC motion globally (*1*) during 1951 to 2010 or over the continental United States since 1901 (*4*). The inconsistency will be discussed later along with the question of whether the observed trends can be attributed to anthropogenic forcing.

For the scenario with strong future anthropogenic warming, the changes of TC motion become pronounced (Fig. 2B). However, the tropical responses of TC motion in the Central Pacific (170°E to 135°W) and Caribbean show opposite signs in the future warming scenario (Fig. 2B) instead of the same sign, as in the historical simulation (Fig. 2A). The pattern differences could occur for a number of reasons, as the SST and circulation patterns of future anthropogenic warming projected by the Coupled Model Intercomparison Project Phase 5 (CMIP5) models can differ from simulated historical changes, as, for example, the changes in various climate forcing agents differ between the historical period and the future projections. Perhaps counterintuitively, the most notable response in Fig. 2B is the extratropical deceleration between 30°N and 45°N (Fig. 2B), which is about 1 m s^{-1} or 15% of the local historical values. The extratropical deceleration not only is evident over the open ocean but also appears in proximity to some populated coastal regions, including Japan and the northeastern United States.

The projected changes of future TC motion are associated with complex changes of the large-scale circulation (Fig. 2D). In the tropics, the midtropospheric circulation is projected to accelerate in parts of the Atlantic and the Pacific. However, these changes differ from the lower tropospheric circulation changes (fig. S2), which show better consistency with the projected responses of TC motion over the tropical central Pacific and the Caribbean. Nonetheless, our confidence in the robustness of the projected tropical changes is relatively low, as the future changes of the tropical SST and circulation are strongly model dependent (*17*, *21*, *32*). In the Northern Hemisphere extratropics, the dominant circulation response is related to a northward displacement of the midlatitude jet, which contributes to a weaker westerly flow between 30°N and 45°N. The flow deceleration extends throughout the troposphere (fig. S2) and is consistent with the deceleration of TC motion in the same region. The projected jet displacement has some mechanism (*33*) and quantitative (*20*, *21*) uncertainties, and the robustness of the projection also differs with seasons and basins, as the radiative forcing and the ocean warming related to greenhouse gas forcings have opposite effects on the displacement of the North Pacific jet during the summertime (*21*, *22*). Nonetheless, the jet displacement, especially in the North Atlantic (June to November) (*21*), has been robustly projected by CMIP5 models (*20*, *21*) and an additional high-resolution climate model that we examined (figs. S4, S6, and S7). The jet displacement has, to date, rarely been connected to future changes of TC activity, but the model consensus helps to increase our confidence in the projected deceleration of TC motion in the extratropics.

Implications for interpreting historical TC motion trends

Here, we further examine the inconsistency between the observed and the simulated historical trends of TC motion (Fig. 3). As suggested by Kossin (*1*), the observational trend during 1951 to 2010 shows a slowdown of TC motion in the zonal average, and the slowdown appears more pronounced in the coastal region of the Northwestern Pacific. In contrast, the simulated historical trend suggests that TC motion has accelerated in the Pacific, but there is a lack of statistically significant signals in the Atlantic region. The model finding raises further questions about the reliability of the observed trends as discussed in previous studies (*2*–*4*, *23*), although the simulated TC responses also have substantial uncertainties (Fig. 3B and fig. S8). But aside from these possibilities, we note that the pattern of the observational trend is noisy (Fig. 3A). This noisiness suggests that internal atmospheric variability, rather than coherent large-scale changes, might have been primarily responsible for the observed trends on the regional scale.

To explore the relative contribution of responses to prescribed historical SST forcing and greenhouse gas changes versus unforced atmospheric variability, we examine the distributions of zonally averaged trends of TC motion and large-scale circulation (Fig. 4). As an approximation, the average of individual ensemble members indicates the modeled forced response, while the spread indicates unforced atmospheric variability. Although more than half of the model realizations show a positive trend of TC motion between 10°N and 40°N, the trends are not significantly different from zero ($P > 0.05$) at nearly all the latitudes. Similarly, over half of the model realizations suggest a positive trend of the large-scale circulation between 15°N and 30°N, but the difference from zero is not statistically significant ($P > 0.05$). The low statistical significance is also suggested by the analysis of large-ensemble simulations by another model (fig. S9). The findings suggest that the signal-to-noise ratio is low in the historical (1951–2010) simulations and that the trend in an individual model realization could easily be dominated by unforced atmospheric variability. The model-simulated unforced atmospheric variability may also be used to assess the observed trend. If one assumes that the model can reliably represent the unforced atmospheric variability of the real world, then the observed trend of TC motion during 1951 to 2010 (Fig. 4A) does not significantly differ from zero ($P > 0.05$), either.

Nonetheless, the unforced atmospheric variability cannot explain all the inconsistencies between the observed and the simulated trends (Fig. 4A). For example, the observed trend is outside the envelope of simulated values at some lower latitudes, underlining the difficulty of reconciling weak changes in the observations and simulations. Our historical (1951–2010) simulations might have biases in the TC response to the imposed SST and greenhouse

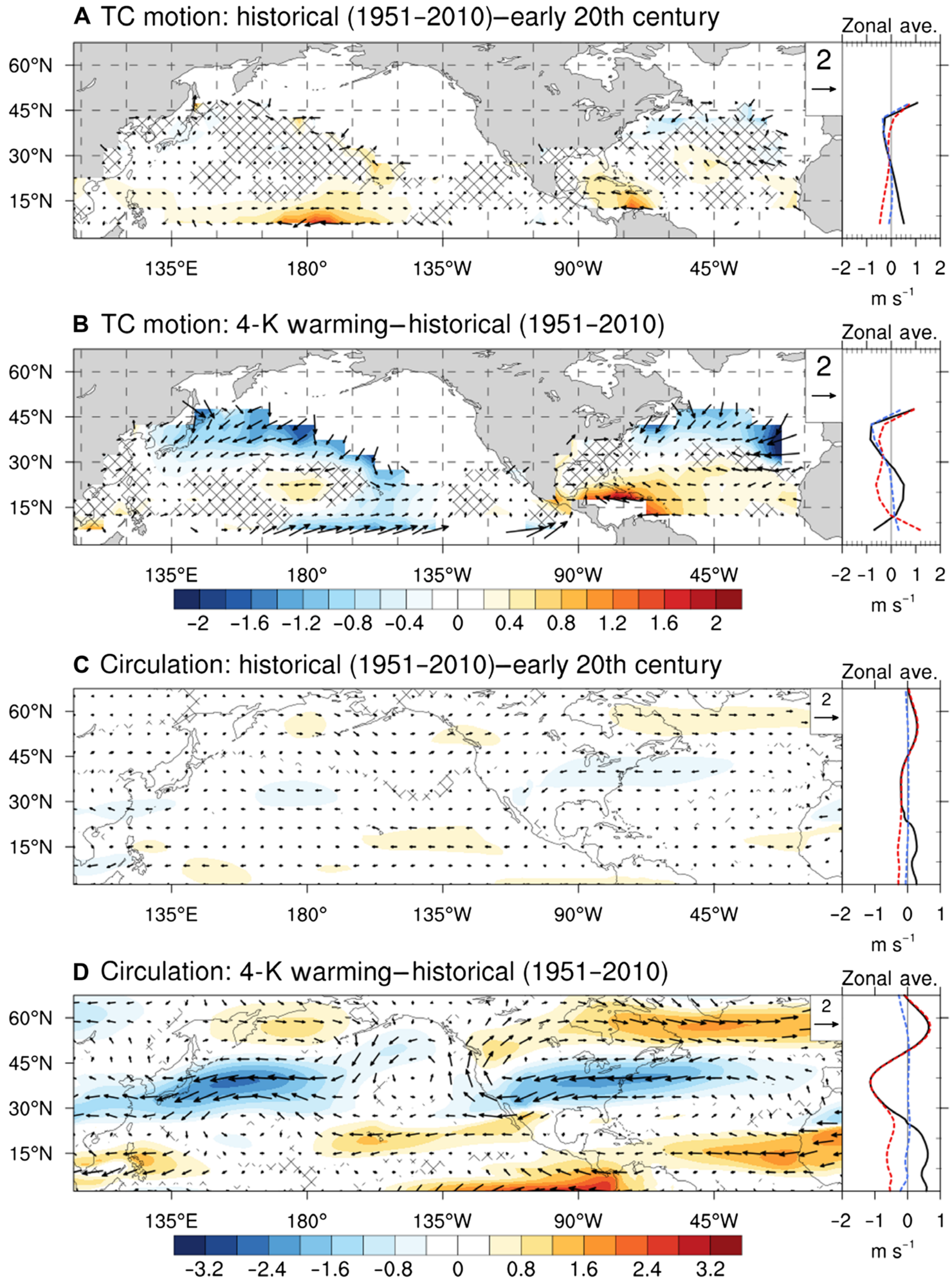

Fig. 2. Simulated changes of TC motion (m s^{-1}) and an approximation for TC-steering circulation (m s^{-1}) July to October. (**A**) TC motion differences between the historical (1951–2010) experiment and the early 20th-century experiment. (**B**) TC motion differences between the 4-K warming experiment and the historical (1951–2010) experiment. (**C**) and (**D**) are the same as (A) and (C), except for showing the midtropospheric (500-hPa) circulation. Color shading depicts differences in translation speed (A and B) or wind speed (C and D). The hatching in the left panels indicates differences are not significant at the 0.05 significance level as determined using a two-sided Student's *t* test. The right panels show the zonally averaged changes of speed magnitude (black), zonal component (red), and meridional component (blue) of TC motion (A and B) and midtropospheric wind (C and D).

gas forcings, uncertainties in these forcing, or underestimated internal atmospheric variability. Another concern is the reliability of observational data. Besides uncertainties in TC data (*2*–*4*, *23*) as previously discussed, the large-scale circulation trends in the observation-based reanalysis datasets may contain artifacts (*19*) or show substantial inconsistency (Fig. 4B). For example, the three datasets that we examined disagree on signs, locations, and magnitudes of the historical circulation changes in some regions. These disagreements also cast doubt on the notion that large-scale circulation changes have driven the observed global trend of TC motion during 1951 to 2010. Nonetheless, there are weak but significant differences in TC motion and atmospheric circulation between the historical (1951–2010) and the early 20th-century experiments (Fig. 2). The evidence suggests that SST variability, together with changes of anthropogenic

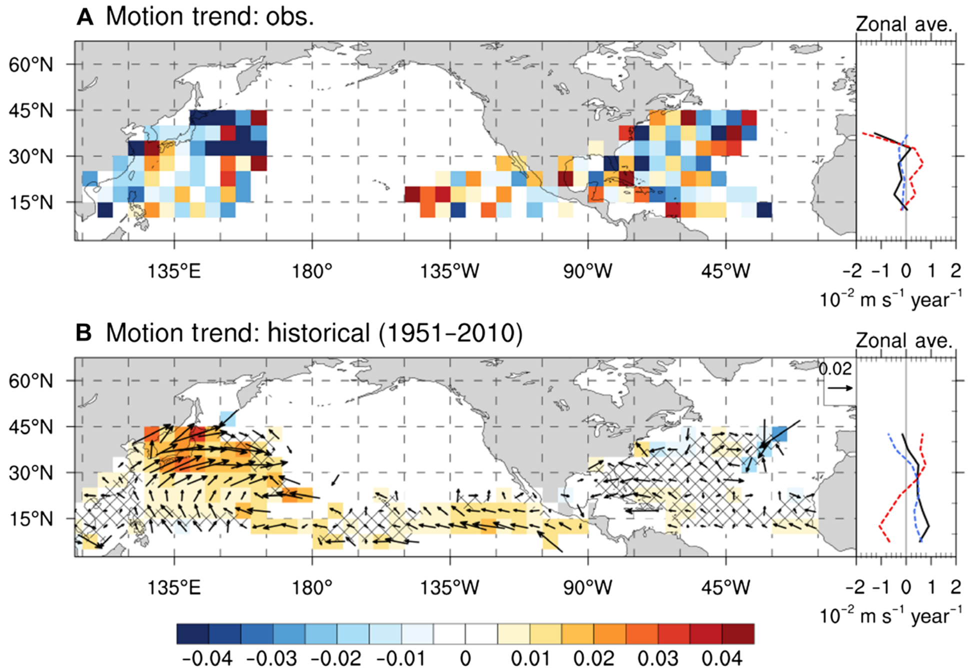

Fig. 3. Observed and simulated trends of TC motion during 1951 to 2010 (m s^{-1}year^{-1}). (**A**) Trend in IBTrACS data. (**B**) Trend in the ensemble average of the historical (1951–2010) simulation. The linear trend calculation is limited to regions where TCs track through in at least 30 of 60 years. Hatching in (B) indicates differences that are not significant at the 0.05 significance level that is determined using a two-sided Student's *t* test. The right panels show the zonally averaged trends of speed magnitude (black), zonal motion vector (red), and meridional motion vector (blue).

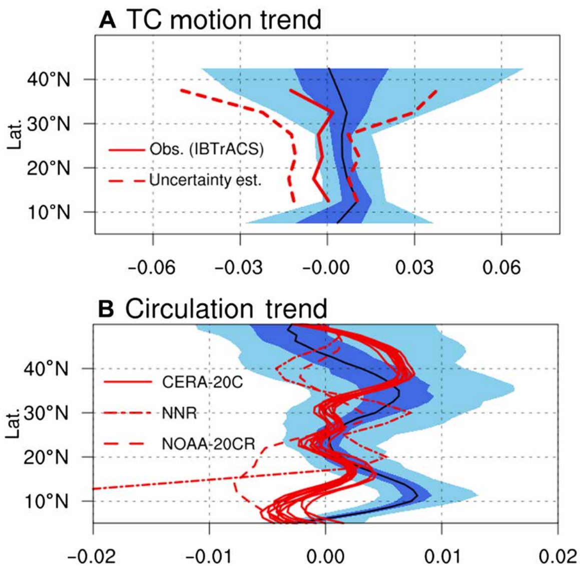

Fig. 4. Zonally averaged trends (1951–2010) in TC motion and the midtropospheric TC-steering circulation within 100°E to 350°E. (**A**) Trend in TC motion (m s^{-1} year^{-1}). (**B**) Trend in midtropospheric (500-hPa) wind speed (m s^{-1} year^{-1}). Light blue shading, dark blue shading, and black line indicate the model-simulated distribution of trends (1951–2010) at the 2.5th/97.5th, 25th/75th, and 50th percentile, respectively. The dashed red lines in (A) indicate estimated uncertainties for the observed trend using the 95% confidence range of the historical simulations (1951–2010). The groups of red lines in (B) show circulation trend values from observation-constrained data, including CERA-20C (10 possible realizations), NNR [National Centers of Environmental Prediction (NCEP)/National Center for Atmospheric Research (NCAR) reanalysis], and NOAA-20CR [National Oceanic and Atmospheric Administration (NOAA) 20th Century Reanalysis version 2c].

forcing, might have at least weakly affected both TC motion and the large-scale circulation.

DISCUSSION

Our analysis of large-ensemble simulations of TC activity suggest that future anthropogenic warming can lead to a robust slowing of TC motion, particularly in the midlatitudes. The slowdown there is related to a poleward shift of the midlatitude westerlies, which has been projected by various climate models. Although not directly examined by this study, the poleward shift of the midlatitude westerlies is also closely related to a poleward shift of extratropical weather perturbations. A reduction of weather perturbations near 30°N has been robustly projected by climate models (*34*) and might contribute to a slowdown of TC motion (*10*). Meanwhile, the historical simulations suggest that the attribution of the observed trends of TC motion to anthropogenic forcings remains uncertain, even though anthropogenic forcings might have weakly affected TC motion and the devastating effects of some recent slow-moving TCs (e.g., Harvey, Florence, Dorian, and Idai) are noteworthy.

The responses of TC motion to the future anthropogenic warming scenario warrant additional remarks. Our warming experiments consider a climate with a constant 4-K warming and constant level of greenhouse gases instead of a climate that experiences a gradual increase of greenhouse gases. It is difficult to estimate when robust and detectable responses are likely to emerge in the real world, partly because the sensitivity of TC motion to anthropogenic forcing has substantial uncertainties. For example, some climate simulations conducted using another model that includes more coupled climate processes (*25*) suggest that the sensitivity of TC motion in the extratropics might be as much as 1 to 1.5 m s^{-1} K^{-1} near 40°N (fig. S3), or about four to six times of the value in Fig. 2D. The differences of sensitivity are likely related to SST warming patterns (e.g., figs. S3 and S7), which modulate the displacement of the midlatitude westerlies on the regional scale (*22*). Nonetheless, all the examined models indicate that strong anthropogenic forcing (e.g., 4-K warming and quadrupling CO_2) can drive substantial changes of TC motion, especially a slowing in the extratropics. The projected extratropical slowing of TC motion, along with the potential increase of TC frequency and intensity (*30*) in the extratropics, might compound TC damages in some of the most populated coastal regions.

METHODS

Model simulation settings

The large-ensemble simulation is part of the Database for Policy Decision Making for Future Climate Change [d4PDF; (*31*)]. The simulation is conducted using Meteorological Research Institute–Atmospheric General Circulation Model version 3.2 (MRI-AGCM3.2H) (*35*) on the TL319 grid, which has ~60-km grid spacing and includes 64 vertical levels throughout the atmosphere. In the historical (1951–2010) simulation, the AGCM is integrated from 1951 to 2010 with the forcing of the observed time-varying SST and sea-ice information, the observed time-varying greenhouse gases, estimated aerosols, and ozone. To generate large-ensemble simulations, the initial conditions of the atmosphere and the observational SST were randomly perturbed. In addition, random SST perturbations up to 30% of the observed interannual variability are added to the observational data to account for observational uncertainties. The resulting variability across ensemble members is referred to as "internal atmosphere variability" in this report. The setup of the early 20th-century simulation is similar, but the simulation uses the 1951 to 2010 boundary conditions that are detrended. Furthermore, the baseline of the SST is set at the early 20th-century level based on a century-scale trend analysis. The greenhouse gas forcing is set at the 1850 level, and the aerosol forcing is set at the estimated preindustrial level. In the future warming simulation, the model is integrated for 60 years with the greenhouse gas forcing set to the values at 2090 of the representative concentration pathway 8.5 (RCP8.5) scenario of CMIP5. Corresponding to the greenhouse gas forcing, the global mean surface temperature is set to be 4 K warmer than that of the preindustrial climate. The 4-K warming is not globally uniform but has patterns based on CMIP5 model RCP8.5 warming experiments. The warming simulations explore potential changes of the SST pattern by using six rescaled change patterns from CMIP5 models. Each of the six CMIP5 warming patterns is used to generate a 15-member ensemble, ultimately leading to a 90-member ensemble of the future climate. More details of the model settings and the experiment design are available in the work of Mizuta *et al.* (*31*).

TC tracking and analysis

The tracking of TCs in the large-ensemble simulation uses 6-hourly model output. The tracking method is the same as described by Murakami *et al.* (*36*) and considers relative vorticity (850 hPa), wind speed (850 hPa), and the cyclone structure. The threshold setting is model and resolution dependent. Specifically, the tracking filters out storms without a warm-core structure, thus excluding the extratropical phase of TCs. We refer interested readers to Murakami *et al.* (*36*) and Yoshida *et al.* (*30*) for more details. The observational TC dataset used in this study is the International Best Track Archive for Climate Stewardship (IBTrACS) dataset (*37*). In contrast to the automatic tracking applied to the large-ensemble simulation, the observational dataset relies on manual analysis by forecasters and researchers. Therefore, the observed track information might be subject to inconsistent standards, subjective analysis errors, and more limited observations in earlier historical periods (*23*). Our analysis excludes the storm systems that were flagged as having undergone extratropical transition and losing their warm-core structure. These posttransition storms, such as Hurricane Sandy (2012), can still be dangerous to coastal communities. When analyzing TC motion, we calculate the motion vectors of TCs that pass near grid points in a 5° latitude-longitude coordinate. To limit spurious noise of motion vectors, our analysis of the observational data and the model output only examine the grid points with a TC-return period (i.e., an average time between TC events) of 20 years or less.

Reanalysis data

We analyze the large-scale circulation using the observation-based reanalysis datasets. These datasets are generated using computer models that are qualitatively similar to the model used in our simulation. However, these reanalysis datasets are further constrained by observations at the surface and/or higher vertical levels. We primarily analyze the ECMWF's Coupled Ocean-Atmosphere Reanalysis of the 20th Century [CERA-20C; (*38*)], which includes 10 individual ensemble members. To highlight the uncertainties in historical circulation trends, we also examine the National Oceanic and Atmospheric Administration (NOAA) 20th Century Reanalysis version 2c [NOAA-20CR; (*39*)] and National Centers of Environmental Prediction (NCEP)/National Center for Atmospheric Research (NCAR) reanalysis [NNR; (*40*)]. CERA-20C and NOAA-20CR are constrained by the surface observations, while the NNR is constrained by both surface and upper-level observations. We chose these reanalysis datasets partly because of their extended temporal coverage, which facilitates the comparison with TC data during 1951 to 2010.

SUPPLEMENTARY MATERIALS

Supplementary material for this article is available at http://advances.sciencemag.org/cgi/content/full/6/17/eaaz7610/DC1

REFERENCES AND NOTES

1. J. P. Kossin, A global slowdown of tropical-cyclone translation speed. *Nature* **558**, 104–107 (2018).
2. I.-J. Moon, S.-H. Kim, J. C. L. Chan, Climate change and tropical cyclone trend. *Nature* **570**, E3–E5 (2019).
3. J. R. Lanzante, Uncertainties in tropical-cyclone translation speed. *Nature* **570**, E6–E15 (2019).
4. J. P. Kossin, Reply to: Moon, I.-J. et al.; Lanzante, J. R. *Nature* **570**, E16–E22 (2019).
5. J. C. L. Chan, The physics of tropical cyclone motion. *Annu. Rev. Fluid Mech.* **37**, 99–128 (2005).
6. G. J. Holland, Tropical cyclone motion: Environmental interaction plus a beta effect. *J. Atmos. Sci.* **40**, 328–342 (1983).
7. W. Ulrich, R. K. Smith, A numerical study of tropical cyclone motion using a barotropic model. II: Motion in spatially-varying large-scale flows. *Q. J. R. Meteorol. Soc.* **117**, 107–124 (1991).
8. R. T. Williams, J. C.-L. Chan, Numerical studies of the beta effect in tropical cyclone motion. Part II: Zonal mean flow effects. *J. Atmos. Sci.* **51**, 1065–1076 (1994).
9. Y. Wang, G. J. Holland, Tropical cyclone motion and evolution in vertical shear. *J. Atmos. Sci.* **53**, 3313–3332 (1996).
10. G. Zhang, T. R. Knutson, S. T. Garner, Impacts of extratropical weather perturbations on tropical cyclone activity: Idealized sensitivity experiments with a regional atmospheric model. *Geophys. Res. Lett.* **46**, 14052–14062 (2019).

11. P.-S. Chu, J.-H. Kim, Y. Ruan Chen, Have steering flows in the western North Pacific and the South China Sea changed over the last 50 years? *Geophys. Res. Lett.* **39**, L10704 (2012).
12. T. R. Knutson, S. Manabe, Time-mean response over the Tropical Pacific to increased CO_2 in a coupled ocean-atmosphere model. *J. Climate* **8**, 2181–2199 (1995).
13. I. M. Held, B. J. Soden, Robust responses of the hydrological cycle to global warming. *J. Climate* **19**, 5686–5699 (2006).
14. E. A. Barnes, L. M. Polvani, CMIP5 projections of Arctic amplification, of the North American/North Atlantic circulation, and of their relationship. *J. Climate* **28**, 5254–5271 (2015).
15. D. Coumou, J. Lehmann, J. Beckmann, The weakening summer circulation in the Northern Hemisphere mid-latitudes. *Science* **348**, 324–327 (2015).
16. J. A. Screen, C. Deser, D. M. Smith, X. Zhang, R. Blackport, P. J. Kushner, T. Oudar, K. E. McCusker, L. Sun, Consistency and discrepancy in the atmospheric response to Arctic sea-ice loss across climate models. *Nat. Geosci.* **11**, 155–163 (2018).
17. B. Xiang, B. Wang, J. Li, M. Zhao, J.-Y. Lee, Understanding the anthropogenically forced change of Equatorial Pacific trade winds in coupled climate models. *J. Climate* **27**, 8510–8526 (2014).
18. E. A. Barnes, J. A. Screen, The impact of Arctic warming on the midlatitude jet-stream: Can it? Has it? Will it? *Wiley Interdiscip. Rev. Clim. Change* **6**, 277–286 (2015).
19. R. Chemke, L. M. Polvani, Opposite tropical circulation trends in climate models and in reanalyses. *Nat. Geosci.* **12**, 528–532 (2019).
20. E. A. Barnes, L. Polvani, Response of the midlatitude jets, and of their variability, to increased greenhouse gases in the CMIP5 models. *J. Climate* **26**, 7117–7135 (2013).
21. I. R. Simpson, T. A. Shaw, R. Seager, A diagnosis of the seasonally and longitudinally varying midlatitude circulation response to global warming. *J. Atmos. Sci.* **71**, 2489–2515 (2014).
22. T. A. Shaw, A. Voigt, Tug of war on summertime circulation between radiative forcing and sea surface warming. *Nat. Geosci.* **8**, 560–566 (2015).
23. G. A. Vecchi, T. R. Knutson, On estimates of historical North Atlantic tropical cyclone activity. *J. Climate* **21**, 3580–3600 (2008).
24. H. Murakami, E. Levin, T. L. Delworth, R. Gudgel, P.-C. Hsu, Dominant effect of relative tropical Atlantic warming on major hurricane occurrence. *Science* **362**, 794–799 (2018).
25. G. A. Vecchi, T. Delworth, R. Gudgel, S. Kapnick, A. Rosati, A. T. Wittenberg, F. Zeng, W. Anderson, V. Balaji, K. Dixon, L. Jia, H.-S. Kim, L. Krishnamurthy, R. Msadek, W. F. Stern, S. D. Underwood, G. Villarini, X. Yang, S. Zhang, On the seasonal forecasting of regional tropical cyclone activity. *J. Climate* **27**, 7994–8016 (2014).
26. E. N. Lorenz, Deterministic nonperiodic flow. *J. Atmos. Sci.* **20**, 130–141 (1963).
27. J. E. Kay, C. Deser, A. Phillips, A. Mai, C. Hannay, G. Strand, J. M. Arblaster, S. C. Bates, G. Danabasoglu, J. Edwards, M. Holland, P. Kushner, J.-F. Lamarque, D. Lawrence, K. Lindsay, A. Middleton, E. Munoz, R. Neale, K. Oleson, L. Polvani, M. Vertenstein, The Community Earth System Model (CESM) large ensemble project: A community resource for studying climate change in the presence of internal climate variability. *Bull. Am. Meteorol. Soc.* **96**, 1333–1349 (2015).
28. W. Mei, Y. Kamae, S.-P. Xie, K. Yoshida, Variability and predictability of North Atlantic hurricane frequency in a large ensemble of high-resolution atmospheric simulations. *J. Climate* **32**, 3153–3167 (2019).
29. G. Zhang, H. Murakami, R. Gudgel, X. Yang, Dynamical seasonal prediction of tropical cyclone activity: Robust assessment of prediction skill and predictability. *Geophys. Res. Lett.* **46**, 5506–5515 (2019).
30. K. Yoshida, M. Sugi, R. Mizuta, H. Murakami, M. Ishii, Future changes in tropical cyclone activity in high-resolution large-ensemble simulations. *Geophys. Res. Lett.* **44**, 9910–9917 (2017).
31. R. Mizuta, A. Murata, M. Ishii, H. Shiogama, K. Hibino, N. Mori, O. Arakawa, Y. Imada, K. Yoshida, T. Aoyagi, H. Kawase, M. Mori, Y. Okada, T. Shimura, T. Nagatomo, M. Ikeda, H. Endo, M. Nosaka, M. Arai, C. Takahashi, K. Tanaka, T. Takemi, Y. Tachikawa, K. Temur, Y. Kamae, M. Watanabe, H. Sasaki, A. Kitoh, I. Takayabu, E. Nakakita, M. Kimoto, Over 5,000 years of ensemble future climate simulations by 60-km global and 20-km regional atmospheric models. *Bull. Am. Meteorol. Soc.* **98**, 1383–1398 (2017).
32. J. Ma, S.-P. Xie, Regional patterns of sea surface temperature change: A source of uncertainty in future projections of precipitation and atmospheric circulation. *J. Climate* **26**, 2482–2501 (2013).
33. Z. Tan, O. Lachmy, T. A. Shaw, The sensitivity of the jet stream response to climate change to radiative assumptions. *J. Adv. Model. Earth Systs.* **11**, 934–956 (2019).
34. E. K. M. Chang, Y. Guo, X. Xia, CMIP5 multimodel ensemble projection of storm track change under global warming. *J. Geophys. Res. Atmos.* **117**, D23118 (2012).
35. R. Mizuta, H. Yoshimura, H. Murakami, M. Matsueda, H. Endo, T. Ose, K. Kamiguchi, M. Hosaka, M. Sugi, S. Yukimoto, S. Kusunoki, A. Kitoh, Climate simulations using MRI-AGCM3.2 with 20-km grid. *J. Meteorol. Soc. Jpn.* **90A**, 233–258 (2012).
36. H. Murakami, Y. Wang, H. Yoshimura, R. Mizuta, M. Sugi, E. Shindo, Y. Adachi, S. Yukimoto, M. Hosaka, S. Kusunoki, T. Ose, A. Kitoh, Future changes in tropical cyclone activity projected by the new high-resolution MRI-AGCM. *J. Climate*, **25**, 3237–3260 (2012).
37. K. R. Knapp, M. C. Kruk, D. H. Levinson, H. J. Diamond, C. J. Neumann, The international best track archive for climate stewardship (IBTrACS). *Bull. Am. Meteorol. Soc.* **91**, 363–376 (2010).
38. P. Laloyaux, E. de Boisseson, M. Balmaseda, J.-R. Bidlot, S. Broennimann, R. Buizza, P. Dalhgren, D. Dee, L. Haimberger, H. Hersbach, Y. Kosaka, M. Martin, P. Poli, N. Rayner, E. Rustemeier, D. Schepers, CERA-20C: A coupled reanalysis of the twentieth century. *J. Adv. Model. Earth Systss.* **10**, 1172–1195 (2018).
39. G. P. Compo, J. S. Whitaker, P. D. Sardeshmukh, N. Matsui, R. J. Allan, X. Yin, B. E. Gleason, R. S. Vose, G. Rutledge, P. Bessemoulin, S. Brönnimann, M. Brunet, R. I. Crouthamel, A. N. Grant, P. Y. Groisman, P. D. Jones, M. C. Kruk, A. C. Kruger, G. J. Marshall, M. Maugeri, H. Y. Mok, Ø. Nordli, T. F. Ross, R. M. Trigo, X. L. Wang, S. D. Woodruff, S. J. Worley, The twentieth century reanalysis project. *Q. J. Roy. Meteorol. Soc.* **137**, 1–28 (2011).
40. E. Kalnay, M. Kanamitsu, R. Kistler, W. Collins, D. Deaven, L. Gandin, M. Iredell, S. Saha, G. White, J. Woollen, Y. Zhu, M. Chelliah, W. Ebisuzaki, W. Higgins, J. Janowiak, K. C. Mo, C. Ropelewski, J. Wang, A. Leetmaa, R. Reynolds, R. Jenne, D. Joseph, The NCEP/NCAR 40-year reanalysis project. *Bull. Am. Meteorol. Soc.* **77**, 437–471 (1996).
41. H. Murakami, G. A. Vecchi, S. Underwood, T. L. Delworth, A. T. Wittenberg, W. G. Anderson, J.-H. Chen, R. G. Gudgel, L. M. Harris, S.-J. Lin, F. Zeng, Simulation and prediction of category 4 and 5 hurricanes in the high-resolution GFDL HiFLOR coupled climate model. *J. Climate* **28**, 9058–9079 (2015).

Acknowledgments
Funding: This study is supported by Princeton University's Cooperative Institute for Modeling the Earth system, through the Predictability and Explaining Extremes Initiative. This study used d4PDF produced with the Earth Simulator jointly by science programs (SOUSEI, TOUGOU, SI-CAT, and DIAS) of the Ministry of Education, Culture, Sports, Science, and Technology (MEXT), Japan. **Author contributions:** G.Z. and H.M. developed the research idea and conducted the analyses. R.M. and K.Y. conducted model simulations. G.Z. wrote the initial draft of the paper. T.R.K., H.M., and other authors made suggestions that helped to improve the presentation and the analyses. **Competing interests:** The authors declare that they have no competing interests. **Data and materials availability:** The IBTrACS data are acquired from National Centers for Environmental Information (www.ncdc.noaa.gov/ibtracs/index.php). The output of the d4PDF large-ensemble simulations is publicly available at the Data Integration and Analysis System (www.diasjp.net/en/). The CERA-20C data are provided by the European Centre for Medium-Range Weather Forecasts (ECMWF; www.ecmwf.int/en/forecasts/datasets/reanalysis-datasets/cera-20c), and the NNR and the NOAA-CIRES 20CR v2c data are available at NOAA/Earth System Research Laboratory (www.esrl.noaa.gov/psd/data/gridded/index.html).

Submitted 7 October 2019
Accepted 30 January 2020
Published 22 April 2020
10.1126/sciadv.aaz7610

Citation: G. Zhang, H. Murakami, T. R. Knutson, R. Mizuta, K. Yoshida, Tropical cyclone motion in a changing climate. *Sci. Adv.* **6**, eaaz7610 (2020).